A-posteriori estimation of error in the quantity of interest for laminated composite plates

Mohite P. M. * and Upadhyay C. S. †

Department of Aerospace Engineering,
Indian Institute of Technology, Kanpur, India 208016.

Abstract

Composites are increasingly used in aerospace industry due their high specific strength. Both critical and non-critical components are fabricated using these materials. An effective design of the components made of composites requires a reliable analysis in order to obtain the critical response quantities (e.g. first-ply failure, buckling etc.). Thus, development of appropriate analysis and design tools for composites is essential. Effective analysis of laminated plate structures requires development of an accurate model and an accurate analysis tool. The composite structures like laminated plates, shells are modelled using classical, shear deformable, zig-zag or hierarchic models. The modelling introduces modelling error (with respect to three-dimensional elasticity) in the analysis. In the present analysis, the model is fixed hence the modelling error is not considered.

Among the various approximation methods, the finite element method is predominantly used. This introduces a discretisation error in the analysis. Hence, the error in the quantity of interest (eg. maximum deflection, stress, buckling load, first ply failure load etc.) is due to the discretisation error. Thus, it becomes important to estimate and control the error in the local quantity of interest within specified tolerances. In the present paper, the issue of estimation of error in local quantity of interest is addressed. It will be shown that the error in local quantity of interest can be expressed in terms of standard elemental error indicators. These indicators are obtained by solving a local problem to get either approximation of error (residual problems) or higher order smoothened solution on the element. The methods of the former type are computationally costlier. And

*Graduate student
†Corresponding author (email: shekhar@iitk.ac.in)

the later methods are comparatively much cheaper and accurate, as will be shown in this paper. In the present paper, several a-posteriori error estimators both for actual as well as auxillary problems are discussed for various ply orientations and stacking sequences. It will be shown that the error in local quantity of interest can be reliably predicted, using the given definition of the local error.

Introduction

Composites are increasingly employed in the manufacture of lightweight components. Thin plate or shell type members are often used in aircraft wing, fuselage or auxillary devices. The inherent heterogeneity in the material properties makes the analysis and design of these components more challenging.

Often, in the analysis or design of laminated structures the critical quantities have to be evaluated accurately, for the given load envelope. The critical quantities of interest are maximum stress, deflection, buckling load, first ply failure load, etc. Shape and topology optimization procedures employ these critical quantities as constraint data (see [1] for example). Obviously, accurate evaluation of the critical data is essential for the success of the optimization procedure. Thus, development of appropriate analysis and design tools for composite structures is essential. The use of finite element methods in the analysis of laminated composite structures is prevalent, especially for plate or shell type structures made of unidirectional composites.

The critical quantities have to be obtained accurately, for the design to be reliable. This requires an adaptive finite element analysis, with control of the error in the various desired response quantities. An a-posteriori estimate of the error in the desired response quantity employs the standard local error estimators (see [2] for details). In order to have complete confidence in the computed solution quantities, reliability of the error estimator is essential, both at the local and global levels. Here, energy norm, buckling load and natural frequency are few examples of globally defined quantities whereas maximum displacement, stress, strain and reaction at support are few examples of locally defined quantities.

Adaptive methods are available in the literature (see [3]- [4]), for the control of the discretisation error. Often, these are based on the control of the energy norm of the error, $||\mathbf{e}||_\Omega$ which is given by $||\mathbf{e}||_\Omega = \sqrt{2\mathcal{U}(\mathbf{e})}$ (where $\mathcal{U}(\mathbf{e})$ is the strain energy of the error). This does not guarantee that the particular data of interest is also accurate (i.e. error is within desired tolerances). Often, critical stress or strain data can have significant error even though the energy norm is within acceptable tolerances.

Some of the authors have worked on the error in the local quantity of interest. In [5], [6] it was shown that the error in the quantity of interest can be given in terms of error in the solution of an auxillary problem. The focus of [5]- [7] was to control the "pollution" error in the quantity of interest.

In the present analysis the plate model is fixed and the issue of modelling error will not be discussed. Also the control of error is not part of this paper. The a-posetriori error estimators based on extrapolation method are discussed followed by estimators for error in the local quantity of interest.

Plate Formulation

Several plate models are available in the literature (see [8]- [9]). For the laminated plates, we employ the model given in [8]. For this model, we have:

$$\mathbf{u}\,(x,y,z) = \left\{ \begin{array}{l} u(x,y,z) \\ v(x,y,z) \\ w(x,y,z) \end{array} \right\} = [\phi(z)]\,\mathbf{U}\,(x,y) \tag{1}$$

where

$$[\phi(z)] = \left[\begin{array}{cccccccccccc} \phi_1(z) & 0 & \phi_3(z) & 0 & 0 & \phi_6(z) & 0 & 0 & \phi_9 & 0 & 0 & \cdots \\ 0 & \phi_2(z) & 0 & \phi_4(z) & 0 & 0 & \phi_7(z) & 0 & 0 & \phi_{10}(z) & 0 & \cdots \\ 0 & 0 & 0 & 0 & \phi_5(z) & 0 & 0 & \phi_8(z) & 0 & 0 & \phi_{11}(z) & \cdots \end{array} \right] \tag{2}$$

and

$$\mathbf{U} = \{U_1(x,y)\,U_2(x,y)\,U_3(x,y)\,\cdots\,U_{11}(x,y)\,\cdots\}^T \tag{3}$$

Note that $U_1(x,y)$, $U_3(x,y)$, $U_6(x,y)$, $U_{11}(x,y), \cdots$ are the in-plane components of the displacement term $u(x,y,z)$. Similarly, $U_2(x,y)$, $U_4(x,y)$, $U_7(x,y)$, $U_{10}(x,y), \cdots$ are the in-plane components for the displacement term $v(x,y,z)$. The in-plane components of the transverse displacement $w(x,y,z)$ are given by $U_5(x,y)$, $U_8(x,y)$, $U_{11}(x,y), \cdots$. In this study only the first eight terms in the expansion will be used (i.e. 8-field model), for which the transverse functions are given in terms of the normalized transverse coordinate $\hat{z} = \frac{2}{t}z$ (where t is the thickness of the laminate), as (see [8] for details):

$$\phi_1(\hat{z}) = \phi_2(\hat{z}) = \phi_5(\hat{z}) = 1, \phi_3(\hat{z}) = \phi_4(\hat{z}) = \hat{z}\,\tfrac{t}{2}$$

$$\phi_6(\hat{z}) = \tfrac{t}{2}\{\varphi(\hat{z}) - \varphi(0)\}, \phi_7(\hat{z}) = \tfrac{t}{2}\{\psi(\hat{z}) - \psi(0)\}$$

$$\phi_8(\hat{z}) = \tfrac{t}{2}\{\rho(\hat{z}) - \rho(0)\}$$

where

$$\varphi(\hat{z}) = \int_{-1}^{\hat{z}} \frac{Q_{44} - Q_{45}}{Q_{44}Q_{55} - Q_{45}^2} d\bar{\hat{z}}; \quad \psi(\hat{z}) = \int_{-1}^{\hat{z}} \frac{Q_{55} - Q_{45}}{Q_{44}Q_{55} - Q_{45}^2} d\bar{\hat{z}}; \quad \rho(\hat{z}) = \int_{-1}^{\hat{z}} \frac{1}{Q_{33}} d\bar{\hat{z}}$$

Where Q_{ij} are the coefficients of the global constitutive relation, in the global xyz-coordinate system.

$$\{\bar{\sigma}_{(l)}\} = [C_{(l)}]\,\{\bar{\epsilon}_{(l)}\} \tag{4}$$

where $\{\bar{\sigma}_{(l)}\} = \{\sigma_{11}^{(l)}\,\sigma_{22}^{(l)}\,\sigma_{33}^{(l)}\,\sigma_{23}^{(l)}\,\sigma_{13}^{(l)}\,\sigma_{12}^{(l)}\}^T$ are the stress components for the layer, and $\{\bar{\epsilon}_{(l)}\} = \{\epsilon_{11}^{(l)}\,\epsilon_{22}^{(l)}\,\epsilon_{33}^{(l)}\,\gamma_{23}^{(l)}\,\gamma_{13}^{(l)}\,\gamma_{12}^{(l)}\}^T$ are the strain components for the layer. Note that here the subscripts $1, 2, 3$ correspond to the three principal material directions. The constitutive relationship in the global xyz - coordinates (for each lamina) can be obtained by the usual transformation to get,

$$\{\sigma_{(l)}\} = [Q_{(l)}]\,\{\epsilon_{(l)}\} \tag{5}$$

with $\{\sigma_{(l)}\} = \{\sigma_{xx}^{(l)}\,\sigma_{yy}^{(l)}\,\sigma_{zz}^{(l)}\,\sigma_{yz}^{(l)}\,\sigma_{xz}^{(l)}\,\sigma_{xy}^{(l)}\}^T$ and the strain $\{\epsilon_{(l)}\} = \{\epsilon_{xx}\,\epsilon_{yy}\,\epsilon_{zz}\,\gamma_{yz}\,\gamma_{xz}\,\gamma_{xy}\}^T$, and $[Q_{(l)}]$ can be obtained from $[C_{(l)}]$ by transformation from the principal material coordinates to the global xyz-coordinates.

The potential energy, Π, for the structure is given by:

$$\Pi = \frac{1}{2}\int_V \{\sigma\}\cdot\{\epsilon\}\,dV - \int_{R^+\cup R^-} q\,w\,ds \tag{6}$$

where V is the volume enclosed by the plate domain, R^+ and R^- are the top and bottom faces of the plate and $q(x, y)$ is the applied transverse load on these faces (see Figure 1).

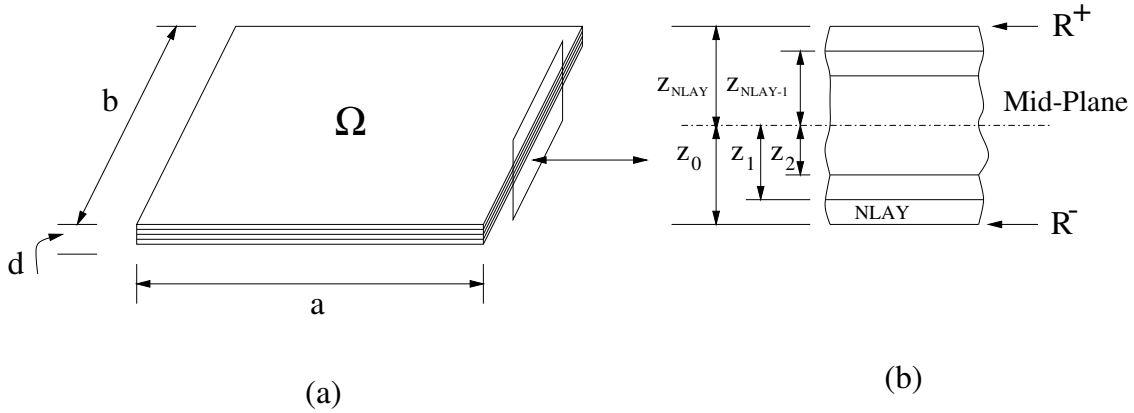

Figure 1: Plate domain with interlaminar interfaces and top and bottom faces.

The solution to the problem, $\mathbf{u}_{ex}$, is the minimizer of the total potential Π, and is given as:

Find $\mathbf{u}_{ex} \in \mathbf{H}^0(V)$ such that

$$B(\mathbf{u}_{ex}, \mathbf{v}) = F(\mathbf{v}) \quad \forall \ \mathbf{v} \in \mathbf{H}^0(V) \tag{7}$$

where $\mathbf{H}^0(V) = \{\mathbf{u} = [\Phi]\mathbf{U} \mid \mathcal{U}(\mathbf{u}) < \infty \text{ and } [\mathbf{M}]\mathbf{U} = \mathbf{0} \text{ on } \Gamma_D\}$. Here $\Gamma = \Gamma_N \cup \Gamma_D$ is the lateral boundary of the plate with the Dirichlet part Γ_D and Neumann part Γ_N. Note that in this study Dirichlet means the parts of the lateral boundary where geometric constraints are imposed, while Neumann stands for the stress-free parts of the lateral boundary. Further, $[\mathbf{M}]$ depends on the type of Dirichlet condition on the edge, i.e. clamped; soft simple-support; hard simple-support etc.

Hence, we have

$$B(\mathbf{u}_{ex},\, \mathbf{v}) = \sum_l B_l\,(\mathbf{u}_{ex},\, \mathbf{v}) = \sum_l \int_{V_l} \{\sigma_{(l)}(\mathbf{u}_{ex})\} \cdot \{\epsilon_{(l)}(\mathbf{v})\}\, dV$$

where V_l is the volume of the l^{th} lamina in the laminate; v_3 is the transverse component of the test function $\mathbf{v}$.

A-posteriori error estimators based on smoothening methods

Definition of a-posteriori error estimator based on strain recovery and displacement recovery

Let $\mathbf{u}_{FE}$ be the finite element solution and $\varepsilon(\mathbf{u}_{FE})$ the corresponding strain components. The a-posteriori estimation of the error is based on the recovery of a smoothened strain field ε^*, or displacement field $\mathbf{u}^*$, by postprocessing $\mathbf{u}_{FE}$. This recovered strain or displacement field is used to define the element error indicator η_τ, which for the element τ is given as:

$$\eta_\tau^2 = \int_\tau \Big(\sum_{i=1}^{NLAY} \int_{z_{i-1}}^{z_i} \big((\varepsilon^* - \varepsilon(\mathbf{u}_{FE})) \cdot \bar{\mathbf{Q}}^{(i)} (\varepsilon^* - \varepsilon(\mathbf{u}_{FE})) \big)\, dz \Big)\, dA \tag{8}$$

where ε^* is obtained either by directly recovering a strain field, or from the recovered displacement field $\mathbf{u}^*$. Several postprocessing procedures are possible (see [10],[11],[13]). The postprocessing procedures employed in this study are:

(a) Estimator based on strain recovery (EST1):

For each element τ, a polynomial strain field $\varepsilon^* \in \mathcal{P}_\varepsilon(\tau)$ is recovered, by using an energy projection of the finite element strain, $\varepsilon(\mathbf{u}_{FE})$, over a one-layer neighbourhood of τ (given as patch P_τ as shown in Figure (2)). This can be represented as:

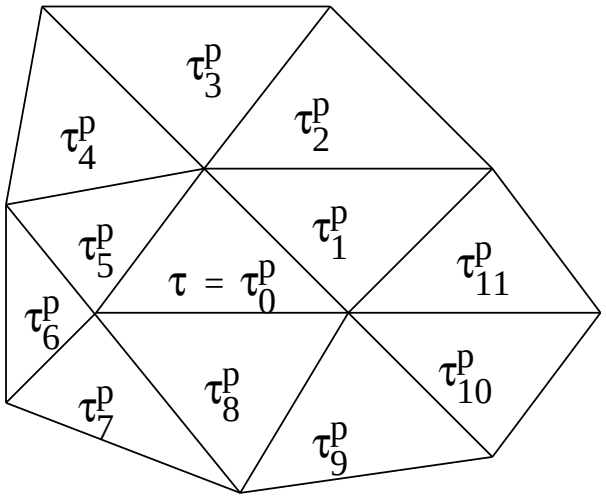

Figure 2: An element τ with a layer of elements $\{\tau_i^P\}_{i=0}^{11}$ surrounding it, forming the patch P_τ.

For element τ, find $\varepsilon^* \in \mathcal{P}_\varepsilon(\tau)$ which minimizes

$$J_{\varepsilon^*} = \frac{1}{2} \sum_{\bar{\tau} \in P_\tau} \sum_{l=1}^{NLAY} \int_{A_{\bar{\tau}}} \int_{z_{l-1}}^{z_l} (\varepsilon^* - \varepsilon(\mathbf{u}_{FE})\,) \cdot \mathbf{Q}^{(l)} (\varepsilon^* - \varepsilon(\mathbf{u}_{FE})\,)\, dz\, dA \tag{9}$$

where $\mathcal{P}_\varepsilon(\tau) = \{\ \varepsilon \mid \varepsilon_{xx}, \varepsilon_{yy}, \gamma_{xy} \in S^p(P_\tau);\ \varepsilon_{zz}, \gamma_{xz}, \gamma_{yz} \in S^{p+1}(P_\tau)\ \}$, with $S^q(P_\tau)$ being the set of polynomials of order q over the patch P_τ.

(b) Estimator based on displacement field recovery using energy projection (EST2 and EST3):

For each element τ a displacement field $\mathbf{u}^* = \Phi \mathbf{U}^*$, where $\mathbf{U}^* \in \mathcal{P}_u^{p+k}(\tau)$, is recovered using an energy projection of the finite element solution $\mathbf{u}_{FE}$ over the patch P_τ. This can be represented as:

For each τ, find $\mathbf{U}^* \in \mathcal{P}_u^{p+k}(\tau)$ which minimizes

$$J_{\mathbf{U}^*} = \frac{1}{2} \sum_{\bar{\tau} \in P_\tau} \sum_{l=1}^{NLAY} \int_{A_{\bar{\tau}}} \int_{z_{l-1}}^{z_l} (\varepsilon(\mathbf{u}^*) - \varepsilon(\mathbf{u}_{FE})\,) \cdot \mathbf{Q}^{(l)} (\varepsilon(\mathbf{u}^*) - \varepsilon(\mathbf{u}_{FE})\,)\, dz\, dA$$
$$+\delta \sum_{\bar{\tau} \in P_\tau} \int_{A_{\bar{\tau}}} |\mathbf{U}^* - \mathbf{U}_{FE}|^2\, dA$$

where δ is a small number ($\delta = 10^{-8}$ has been used in the study); $\mathcal{P}_u^{p+k}(\tau) = \{\ \mathbf{U} \mid U_i \in S^{p+k}(P_\tau), i = 1, 2, \cdots NMODEL\ \}$; $\mathbf{u}_{FE} = \Phi \mathbf{U}_{FE}$.

The above definition is employed for all elements τ in the interior of the domain for both estimators EST2 and EST3. For EST2, the above definition is also employed for elements at the boundary. However, at boundaries with Dirichlet condition, one would like to impose the applied displacement boundary conditions stringently, while finding $\mathbf{U}^*$. Thus, in the case of EST3, for elements τ at the Dirichlet boundary, $\mathbf{U}^*$ is obtained by minimising:

$$J_{1,\mathbf{U}^*} = J^*_{\mathbf{U}} + \lambda \sum_{\bar{\tau} \in P_\tau} \int_{\partial \bar{\tau} \subseteq \Gamma_D} |\mathbf{U}^* - \bar{\mathbf{U}}|^2 \, ds \tag{10}$$

where λ is a penalty parameter ($\lambda = 10^8$ was employed in the study); $\bar{\mathbf{U}}$ is the known boundary displacement, and Γ_D is the Dirichlet part of the boundary $\partial\Omega_{2D}$ of the domain Ω_{2D}.

(c) Estimator based on displacement field recovery using L_2 projection (EST4):

For each element τ a polynomial displacement field $\mathbf{U}^* \in \mathcal{P}_u^{p+k}(\tau)$ is recovered from the following minimisation problem:

For each τ, find $\mathbf{U}^* \in \mathcal{P}_u^{p+k}(\tau)$ which minimizes

$$J_{2,\mathbf{U}^*} = \frac{1}{2} \sum_{\bar{\tau} \in P_\tau} \int_{A_{\bar{\tau}}} |\mathbf{U}^* - \mathbf{U}_{FE}|^2 dA \tag{11}$$

The estimator obtained with $p+1$ recovery will be referred to as EST4A, while the estimator obtained with $p+2$ recovery will be referred to as EST4B.

Remark : This recovery is a planar recovery, using the L_2 projection of each component of $\mathbf{U}_{FE}$. This leads to very small matrix problems at the element level, with multiple right hand sides. Thus, this recovery is computationally inexpensive.

The detailed procedures for the construction of the various recovery based error estimators is given in the appendix.

The error estimators proposed here have to be tested for their reliability. Since the goal of all smoothening based error estimators is to get superconvergent stress or strain fields, an obvious choice for the measure of the base error (i.e. the desired "true" error) is given as $\mathbf{e} = \mathbf{u}_{FE}^{(p+q)} - \mathbf{u}_{FE}^{(p)}$, with $\mathbf{u}_{FE}^{(k)}$ as the finite element solution with elements of order k.

Given the element error indicators η_τ, the global error estimator ξ_Ω is given as:

$$\xi_\Omega = \sqrt{\sum_{\tau=1}^{NEL} \eta_\tau^2} \tag{12}$$

where NEL is the total number of elements in the mesh.

Thus, the "desired" error norm will be $|||\mathbf{e}|||_\Omega = \sqrt{2\mathcal{U}(\mathbf{e})}$, which will be used to obtain a measure of the quality of the error estimators, i.e.

$$\kappa_\Omega = \frac{\xi_\Omega}{|||\mathbf{e}|||_\Omega} \tag{13}$$

where κ_Ω is the global effectivity index (the ideal value of κ_Ω is 1). The local quality of an estimator will be obtained by finding the effectivity index for the patch ω of interest, i.e.

$$\kappa_\omega = \frac{\xi_\omega}{|||\mathbf{e}|||_\omega} \tag{14}$$

where $\xi_\omega = \sqrt{\sum_{\tau\in\omega}\eta_\tau^2}$, $|||\mathbf{e}|||_\omega = \sqrt{2\,\mathcal{U}_\omega(\mathbf{e})}$ with $\mathcal{U}_\omega(\mathbf{e})$ as the strain energy of the error in the patch ω.

Validation of the quality of a-posteriori error estimators

The effect of all these factors on the local and global quality of a-posteriori error estimators will be studied through numerical examples. The material of interest will be T300/5208 Graphite/Epoxy (prepreg) with the following properties (as given in [14]):

$E_{ll} = 132.5$ GPa; $E_{tt} = 10.8$ GPa; $\nu_{lt} = 0.24$;
$\nu_{tt} = 0.49$; $G_{lt} = 5.7$ GPa; $G_{tt} = 3.4$ GPa

For the numerical study, we will take the plate model given by (4). Further, we will consider only the following types of boundary conditions:

(1) Soft simple support ($u_t = w = 0$), called SS.

(2) Hard simple support ($u_n = w = 0$), called HSS.

(3) Clamped ($u_t = u_n = w = 0$).

where u_t and u_n are the in-plane tangential and normal displacement components, respectively (as shown in Figure (3)); w is the transverse displacement. Here, we will assume the same boundary condition type on all boundary edges.

Case 1: *Quality for element patches in the interior of the domain,* $\Omega_{2D,interior}$

The local performance of the error estimator has to be understood for the various possible scenarios separately. We know that the boundary layer effect in the finite element

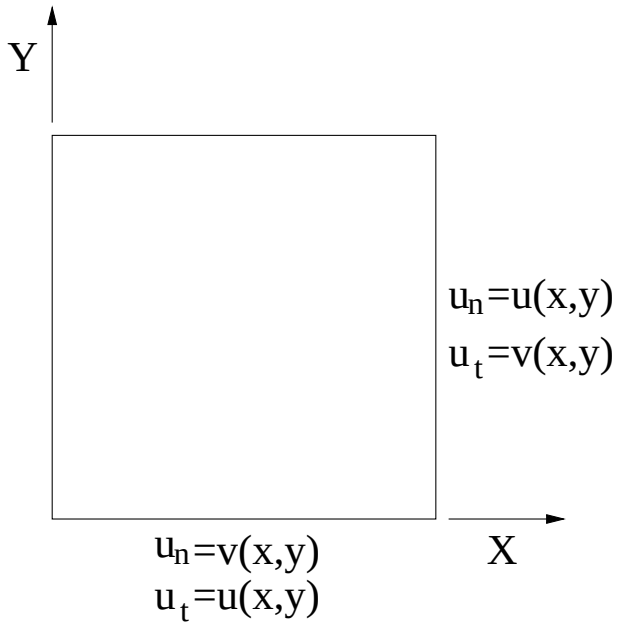

Figure 3: Plate showing tangential and normal components of displacement on the edges.

solution may be present only in few layers of elements adjoining the boundary. For elements removed from the boundary, the finite element solution behaves like the local best approximation, i.e. the local error converges at the optimal rate. Thus, the first check for the quality of the error estimator should be for elements in the interior of the domain, i.e. for element patches (various representative patches are shown in Figure (5)) in the subregion $\Omega_{2D,interior}$. In Figure (4) the element patches at the boundary and interior are shown for the meshes used in this study.

All the numerical results presented will be for the four-layered laminates, unless otherwise specified, with the ply thickness fixed to $d_l = 0.127$ mm, l = 1,2,3, $\cdots$ NLAY. In Tables (1)-(2), the extremal values of the effectivity index (κ_{max}, and κ_{min} respectively), for the element patches ω in the interior of the domain (see Figure (4)) are given for various ply orientations and boundary conditions. Effect of plate thickness is accounted for by taking $\frac{a}{d} = 5$ (thick plate), 10 (moderately thick plate), 100 (thin plate). Elements of order $p = 2$ are taken for thick and moderately thick plates, Note that since we are interested in the asymptotic quality of error estimators, for thin plates $p = 3$ is employed in all cases (as for $p = 2$ the error is not asymptotic in nature). The transverse load is fixed to a uniformly distributed load of intensity $q^+ = 2N/mm^2$ and $q^- = 0$.

From the results we observe that:

(1) Estimators EST1, EST2 and EST4B are very reliable for patches in the interior of

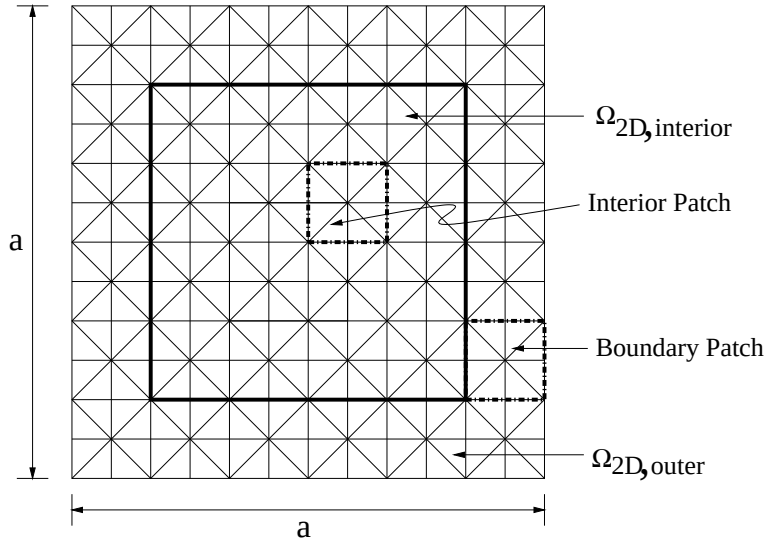

Figure 4: The square plate of dimensions a×a, with the mesh shown. The layer of element patches adjacent to the boundary are given by $\Omega_{2D,outer}$. All other patches lie in subdomain $\Omega_{2D,interior}$. Sample inner and boundary patches are also shown (with dashed border).

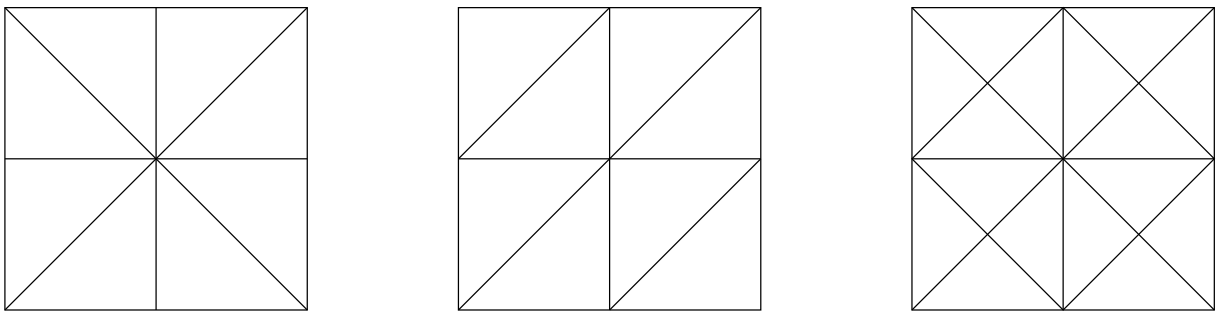

Figure 5: The periodic patterns representing a patch of elements (a) Union Jack (b) Regular (c) Criss-cross.

the domain, with $0.97 \leq \kappa_\omega \leq 1.07$.

(2) The asymptotic quality of error estimators is relatively insensitive to the ply orientation, and plate thickness.

(3) The effect of the boundary conditions is not seen in the interior patches. Hence, the boundary-layer in the numerical solution is localised to only one patch of elements, adjacent to the boundary i.e. elements in $\Omega_{2D,outer}$.

(4) The estimator EST4A is not reliable ($0.98 \leq \kappa_\omega \leq 2.29$). Hence, L_2 projection with (p+1) order polynomials is not advisable. EST4B ($\kappa_\omega \approx 1$) is very reliable in the interior. Hence, L_2 projection with (p+2) order polynomials is more robust.

(5) For interior patches EST2 and EST4B show similar behavior.

Thus, for interior patches EST4B is preferable because it is very robust and the computational cost is negligible, as compared to EST1 and EST2.

Table 1: Quality of error estimators for patches in $\Omega_{2D,interior}$: uniform transverse load ($q^+ = 2N/mm^2$) $[0/90]_s$ laminate.

$\frac{a}{d}$ ratio	Estimator	SSS		HSS		Clamped	
		κ_{min}	κ_{max}	κ_{min}	κ_{max}	κ_{min}	κ_{max}
5	EST1	1.0056	1.0056	1.0175	1.0175	1.0173	1.0173
	EST2	0.9989	0.9989	1.0015	1.0015	1.0014	1.0014
	EST4A	1.0365	1.0365	1.0609	1.0609	1.0604	1.0604
	EST4B	0.9954	0.9954	0.9978	0.9978	0.9976	0.9976
10	EST1	1.0053	1.0053	1.0230	1.0230	1.0231	1.0231
	EST2	1.0014	1.0014	1.0045	1.0045	1.0046	1.0046
	EST4A	1.0713	1.0713	1.1178	1.1178	1.1176	1.1176
	EST4B	1.0003	1.0003	0.9998	0.9998	0.9997	0.9997
100	EST1	1.0025	1.0025	1.0230	1.0230	1.0231	1.0231
	EST2	1.0013	1.0013	0.9958	0.9958	0.9957	0.9957
	EST4A	1.1539	1.1539	1.7105	1.7105	1.7105	1.7105
	EST4B	0.9843	0.9843	0.9789	0.9789	0.9789	0.9789

Case 2: *Quality for element patches in the boundary region, $\Omega_{2D,outer}$*

The local quality of the proposed error estimators are investigated separately for element patches in $\Omega_{2D,outer}$. From the results given in Tables (3)-(4), we observe that:

(1) Estimator EST1 is reliable upto the boundary for all $\frac{a}{d}$ ratios and symmetric cross ply ($[0/90]_s$), with $0.86 \leq \kappa_\omega \leq 1.04$.

Table 2: Quality of error estimators for patches in $\Omega_{2D,interior}$: uniform transverse load ($q^+ = 2N/mm^2$) $[45/-45]_s$ laminate.

$\frac{a}{d}$ ratio	Estimator	SSS		HSS		Clamped	
		κ_{min}	κ_{max}	κ_{min}	κ_{max}	κ_{min}	κ_{max}
5	EST1	1.0203	1.0547	1.0137	1.0719	1.0144	1.0175
	EST2	0.9657	0.9753	0.9807	0.9933	0.9945	0.9986
	EST4A	1.0243	1.0413	1.0419	1.1165	1.0555	1.0855
	EST4B	0.9651	0.9671	0.9755	1.0111	0.9985	1.0025
10	EST1	0.9848	0.9896	0.9892	0.9900	1.0153	1.0193
	EST2	0.9589	0.9777	0.9628	0.9692	0.9959	1.0011
	EST4A	1.0463	1.0469	1.0672	1.1733	1.0919	1.2109
	EST4B	0.9716	0.9743	0.9633	0.9844	0.9888	1.0195
100	EST1	0.9272	0.9307	0.9156	0.9358	0.9900	1.0011
	EST2	0.9305	0.9393	0.9066	0.9243	0.9774	0.9911
	EST4A	0.9863	1.1679	1.3676	2.2956	1.4543	2.5316
	EST4B	0.9217	0.9252	0.9218	0.9323	0.9864	1.0080

(2) For the angle ply laminate ($[45/-45]_s$), the quality of EST1 deteriorates with $0.73 \leq \kappa_\omega \leq 1.70$.

(3) For $[0/90]_s$ laminate with soft simply supported boundary condition, estimators EST1, EST3, EST4B are robust upto the boundary.

(4) Estimator EST3 is better than estimator EST2 for boundary patches. Thus, explicit imposition of the essential boundary conditions is necessary, for the displacement recovery method, in order to get reliable error estimators.

(5) Estimator EST4B is more reliable than EST3. Hence, for the class of problems considered here, estimator EST4B is preferable to EST3.

(6) All estimators can significantly underestimate the error, with $\kappa_{min} \approx 0.6$.

It should be noted that the patches at the boundary correspond to one layer of elements at the domain boundary. Hence, the inferior performance of the estimators (with respect to interior patches) is restricted to a small region abutting the boundary.

Table 3: Quality of error estimators for patches in $\Omega_{2D,outer}$: uniform transverse load ($q^+ = 2N/mm^2$); $[0/90]_s$ laminate.

$\frac{a}{d}$ ratio	Estimator	SSS		HSS		Clamped	
		κ_{min}	κ_{max}	κ_{min}	κ_{max}	κ_{min}	κ_{max}
5	EST1	0.9981	1.0456	0.9668	1.1268	0.9655	1.1195
	EST2	0.9767	1.0211	0.8442	1.0229	0.8468	1.0227
	EST3	0.9838	1.1042	0.8558	1.0229	0.8564	1.0631
	EST4A	0.9699	1.1439	0.9097	1.1262	0.9117	1.1602
	EST4B	0.9621	1.0544	0.8596	1.0086	0.8617	1.0081
10	EST1	0.9845	1.0286	0.8744	1.0691	0.8737	1.0692
	EST2	0.9737	1.0053	0.7988	1.0128	0.8007	1.0128
	EST3	0.9813	1.0293	0.8132	1.0128	0.8564	1.0631
	EST4A	0.9690	1.1186	0.8621	1.2280	0.8633	1.2255
	EST4B	0.9616	1.0382	0.8105	0.9997	0.8124	0.9997
100	EST1	0.9718	1.0209	0.8604	1.0357	0.8617	1.0358
	EST2	0.9689	1.0294	0.6988	1.0178	0.7015	1.0178
	EST3	0.9715	1.0572	0.7211	1.0616	0.7239	1.0853
	EST4A	1.4484	2.6835	1.7091	3.4468	1.4028	3.4483
	EST4B	0.9812	1.3339	0.8395	1.1053	0.7024	1.1035

Table 4: Quality of error estimators for patches in $\Omega_{2D,outer}$: uniform transverse load ($q^+ = 2N/mm^2$); $[45/-45]_s$ laminate.

$\frac{a}{d}$ ratio	Estimator	SSS		HSS		Clamped	
		κ_{min}	κ_{max}	κ_{min}	κ_{max}	κ_{min}	κ_{max}
5	EST1	0.9703	1.7028	0.9462	1.6029	0.9521	1.2558
	EST3	0.8605	2.0219	0.7995	1.8825	0.8356	1.8446
	EST4A	0.9118	1.8953	0.8611	1.7498	0.8911	1.2967
	EST4B	0.8576	1.7705	0.8094	1.6602	0.8445	1.1505
10	EST1	0.8803	1.5212	0.8212	1.2944	0.8673	1.1035
	EST3	0.7796	1.8136	0.7259	1.4505	0.7861	1.5711
	EST4A	0.8557	1.6777	0.7795	1.3885	0.8396	1.3133
	EST4B	0.7651	1.5078	0.7183	1.2323	0.7867	1.0195
100	EST1	0.7331	1.2225	0.8257	1.0354	0.9258	1.0325
	EST3	0.5706	1.5167	0.6118	1.2022	0.8124	1.4295
	EST4A	0.9980	4.0447	0.9276	3.6262	1.4791	3.9337
	EST4B	0.6136	1.3099	0.6111	1.1072	0.8378	1.2803

The Auxillary Problem

Let us consider the domain of figure 6. Let us further assume that we are interested in the value of stress component σ_{xx} in the topmost layer, for all points in the element τ (shown shaded in figure 6).

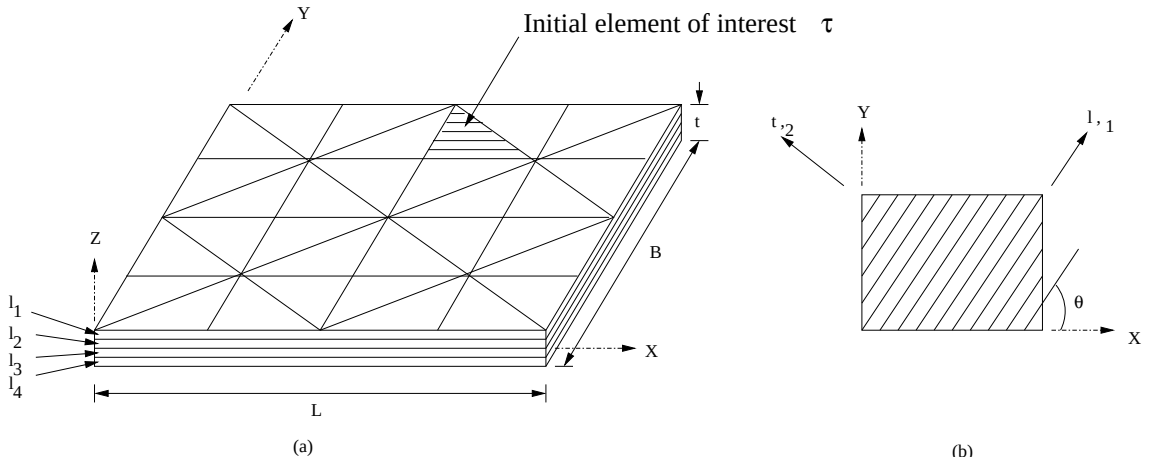

Figure 6: (a) Laminated plate with initial mesh T and element of interest τ. (b) Lamina with material coordinates l, t (or 1, 2)

In order to accurately obtain the pointwise information in τ, we will let $\sigma^{(l)}_{xx,avg} = \frac{1}{v^l_\tau}\int_{v^l_\tau} \sigma_{xx} dv$ as the quantity of interest. Here $v^l_\tau = A_\tau t_l$ is the volume enclosed by the element τ in the l^{th} layer. Hence,

$$\sigma^{(l)}_{xx,avg} = \frac{1}{A_\tau t_l} \int_{z=z_{l-1}}^{z_l} \int_{A_\tau} (\sigma_{xx}\, dA)\, dz \tag{15}$$

with t_l as the thickness of the l^{th} layer; z_{l-1} and z_l as the lower and upper z coordinate for the l^{th} layer; A_τ is the area of element τ.

Remark: Using the average stress in an element, as the quantity of interest, is allowable. This is because control of error in the average stress will ensure accurate values of the pointwise stresses, for all points in the element τ. Further, taking the average over the layer ensures that the stress at all points within the layer will be accurately obtained. We could have taken a slice of the layer (in the vicinity of the interface, for example), as the volume of interest.

Corresponding to $\sigma^{(l)}_{xx,avg}$ we define the following auxillary problem:

Find $\mathbf{G} \in \mathbf{H}^0(V)$ such that

$$B(\mathbf{G}, \mathbf{v}) = \sigma^{(l)}_{xx,avg}(\mathbf{v}) = \mathcal{F}(\mathbf{v}) \quad \forall \ \mathbf{v} \in \mathbf{H}^0(V) \tag{16}$$

Letting $\mathbf{G}_h \in \mathbf{H}^0_h(V)$ be the finite element solution for $\mathbf{G}$, we have

$$B(\mathbf{G}_h, \mathbf{v}_h) = \sigma^{(l)}_{xx,avg}(\mathbf{v}_h) = \mathcal{F}(\mathbf{v}_h) \quad \forall \ \mathbf{v}_h \in \mathbf{H}^0_h(V) \tag{17}$$

Note that letting the approximation for $\mathbf{G}$ to be of the same order, p, as $\mathbf{u}_h$, the auxillary problem gives rise to an additional load vector. Hence, any direct solver, with capability to handle multiple load vectors, can be employed to solve for $\mathbf{u}_h$ and $\mathbf{G}_h$ simultaneously. Further, it should be noted that the same procedure can be carried out for any stress component σ_i, or strain component ϵ_i, displacement $\mathbf{u}$ etc. Simultaneously, all the desired components can be solved for without increasing the computational cost significantly.

Estimators for error in quantity of interest

From the previous section we have:

$$B(\mathbf{G},\ \mathbf{u}_{ex} - \mathbf{u}_h) = \mathcal{F}(\mathbf{u}_{ex}) - \mathcal{F}(\mathbf{u}_h) = \mathcal{F}(\mathbf{u}_{ex} - \mathbf{u}_h) = \mathcal{F}(\mathbf{e}) \tag{18}$$

$$|B(\mathbf{G} - \mathbf{G}_h,\ \mathbf{u}_{ex} - \mathbf{u}_h)| = |\mathcal{F}(\mathbf{e})| \tag{19}$$

or

$$\begin{array}{rcl} |\mathcal{F}(\mathbf{e})| = |B(\mathbf{G} - \mathbf{G}_h, \mathbf{u}_{ex} - \mathbf{u}_h)| & \leq & \sum_\tau |B(\mathbf{G} - \mathbf{G}_h, \mathbf{u}_{ex} - \mathbf{u}_h)| \\ \leq \ \sum_\tau ||\mathbf{e_u}||_\tau \, ||\mathbf{e_G}||_\tau & \leq & ||\mathbf{e_u}||\,||\mathbf{e_G}|| \end{array} \tag{20}$$

where $\mathbf{e_u} = \mathbf{e}$ stands for the error in the actual solution and $\mathbf{e_G}$ stands for the error in the auxillary problem. Thus, we can see that the smoothness of both $\mathbf{u}$ and $\mathbf{G}$ affect the measure of error in the quantity of interest.

Definition of a-posteriori error estimators for local quantity of interest

Replacing $\mathbf{e_u}$ with the estimate $\mathbf{e^*_u}$ and $\mathbf{e_G}$ with the estimate $\mathbf{e^*_G}$, we can get the following definitions of the estimators, for the error in the quantity of interest:

(1) Estimator 1 (E_1):

$$|\mathcal{F}(\mathbf{e})|_{E_1} = |\sum_\tau B(\mathbf{e^*_u}, \mathbf{e^*_G})| \tag{21}$$

(2) Estimator 2 (E_2):

$$|\mathcal{F}(\mathbf{e})|_{E_2} = \sum_\tau |B(\mathbf{e^*_u}, \mathbf{e^*_G})| \tag{22}$$

(3) Estimator 3 (E_3):

$$|\mathcal{F}(\mathbf{e})|_{E_3} = \sum_{\tau} ||\mathbf{e}^*_{\mathbf{u}}|| \; ||\mathbf{e}^*_{\mathbf{G}}|| \tag{23}$$

Remark: Estimators E_2 and E_3 will be more conservative, as compared to E_1. Note that in the definition E_1, the signs of the elemental contributions to the total error can be different, leading to cancellations. However, from the error estimation and adaptivity point of view, we would like to control the intensity (or magnitude) of the elemental contributions to the error in the quantity of interest. This will ensure a uniform decrease in the pointwise errors at a point, or in an element.

Numerical study of the quality of a-posteriori error estimators

The quality of the error estimator, for the quantity of interest, has to be ascertained. In this study we will use the L_2 projection based estimators $\mathbf{e}^*_{\mathbf{u}}$ and $\mathbf{e}^*_{\mathbf{G}}$ (given by definitions (9) and (10)). For this choice of the a-posteriori error estimator we have to determine the quality of the three definitions of the focussed error estimators E_1, E_2 and E_3.

In order to study the reliability of the error estimators, we let $\mathbf{u}_h^{(p)}$, $\mathbf{G}_h^{(p)}$ be the finite element solutions of the order p for $\mathbf{u}_{ex}$ and $\mathbf{G}$. Thus, we can approximate error $\mathbf{e}_{\mathbf{u}}$ as $\mathbf{e}_{\mathbf{u}} \approx \mathbf{e}_{\mathbf{u}}^{(p+1)} = \mathbf{u}_h^{(p+1)} - \mathbf{u}_h^{(p)}$ and hence $\mathcal{F}(\mathbf{e}) \approx \mathcal{F}(\mathbf{e}_{\mathbf{u}}^{(p+1)})$. It can be shown that $\mathcal{F}(\mathbf{e}_{\mathbf{u}}^{(p+1)}) = \sum_\tau B\,(\,\mathbf{e}_{\mathbf{G}}^{(p+1)}, \mathbf{e}_{\mathbf{u}}^{(p+1)}\,)$. With this definition of the "exact" error, we let the effectivity index for the quantity of interest $\kappa_{\mathcal{F}}$ be defined as:

$$\kappa_{\mathcal{F}} = \frac{|\,\mathcal{F}(\mathbf{e}^*)\,|_{E_i}}{|\,\mathcal{F}(\mathbf{e})\,|_{E_i}} \qquad i = 1, 2, 3 \tag{24}$$

Letting τ be the element of interest and P the one-layer neighborhood of τ, the total error can be partitioned into two parts as follows:

$$|\mathcal{F}(\mathbf{e})| \leq |\mathcal{F}_1(\mathbf{e})| + |\mathcal{F}_2(\mathbf{e})|$$

where

$$\mathcal{F}_1(\mathbf{e}) = \sum_{\tau \in P} B(\mathbf{e}_{\mathbf{u}}, \mathbf{e}_{\mathbf{G}}), \quad \mathcal{F}_2(\mathbf{e}) = \sum_{\tau \in P'} B(\mathbf{e}_{\mathbf{u}}, \mathbf{e}_{\mathbf{G}}) \tag{25}$$

where P' is the set of elements lying outside P. Following [5], $\mathcal{F}_1(\mathbf{e})$ is the local part of the error and $\mathcal{F}_2(\mathbf{e})$ is the "pollution" in the quantity of interest (i.e. far-field influence). For each of these quantities, we can obtain the effectivity indices $\kappa_{\mathcal{F}_1}$ and $\kappa_{\mathcal{F}_2}$, by suitably modifying definition (20).

Remark: The significant part of the true error can be given in terms of the $(p+1)$ part of the error, when the pollution (or far-field influence) is not significant (see [12]). The far-field effect is significant when reentrant corners are present in the domain.

Remark: Note that $\mathbf{G}$ is badly behaved in P. Hence, $\mathbf{e_G}$ does not converge locally. Thus, in P $\mathbf{e_G}$ is not approximated well by $\mathbf{e_G^{(p+1)}}$. This means that in P, $\mathbf{e_G^*}$ (or the estimated error) is not a reliable estimate of $\mathbf{e_G}$. However, in the numerical procedure we employ $\mathbf{e_G^*}$ instead of $\mathbf{e_G}$. It will be observed, in the numerical examples that the estimator is still reasonably robust.

We consider the following rectangular laminated plate configuration:

Length $L = 10\,cm$; Breadth $B = 10\,cm$;
Thickness $t = 1\,cm$ (moderately thick plate) or $t = 1\,mm$ (thin plate)
Number of lamina, $NLAY = 4$ (of equal thickness)
$E_{ll} = 138\,MPa \quad E_{tt} = 9.3\,MPa \quad \nu_{lt} = 0.3 \quad \nu_{tt} = 0.5$
$G_{lt} = 4.6\,MPa \quad G_{tt} = 3.1\,MPa$
Loading: Uniformly distributed transverse loading on R^+, $q(x, y) = 100\,kPa$

Here l denotes the fibre direction, for a lamina, and t denotes the transverse direction (see figure 6).

For the plate configuration we consider the following boundary conditions :

Clamped - clamped (CCCC): For $x = 0, L \;\; y = 0, B \;\; u = v = w = 0$
Clamped -free (CFCF): For $x = 0, L \;\; u = v = w = 0$
Simply-supported (SSSS): For $x = 0, L \;\; v = w = 0$; For $y = 0, B \;\; u = w = 0$

Laminates with material orientation of $[0/90/90/0]$ and $[-45/45/45/-45]$ were considered in the numerical examples. Further, it should be noted that in all the examples, the stress quantities have units of kPa. Quadratic finite element approximations ($p = 2$) are employed throughout this study. The order of approximation, p, will be specifically mentioned wherever p other than 2 is employed.

In table 5 and 6 we report the value of $\mathcal{K}_{\mathcal{F}}$ (for total error) and $\mathcal{K}_{\mathcal{F}_2}$ (for pollution error) for a thin plate. We observe that:

(1) Estimator E_1 is not reliable.

(2) Estimator E_3 is very robust ($1.04 \leq \mathcal{K}_{\mathcal{F}} \leq 2.05$), but estimator E_2 can underestimate the error (especially for the $[-45/45/45/-45]$ laminate), with $\kappa_{\mathcal{F}} \geq 0.55$.

(3) Estimator E_1 is sensitive to the boundary condition. E.g. for SSSS underestimation is severe. However, E_2 and E_3 are insensitive to the boundary-condition type.

(4) In the region P', E_1 is completely unreliable with $0.06 \leq \kappa_{\mathcal{F}_2} \leq 46.0$. Estimators E_2 and E_3 are robust in P'.

(5) The error in the quantity of interest can be very high ($> 50\%$), for the mesh shown in figure 6.

Table 5: Quality of Estimator for [0/90/90/0]; plate dimension: $10 \times 10 \times 0.1$

Quantity	B. C.	$\kappa_{\mathcal{F}}$			$\kappa_{\mathcal{F}_2}$			% error
		E_1	E_2	E_3	E_1	E_2	E_3	
$\sigma^{(1)}_{xx,avg}$=-96.05	CCCC	0.92	0.87	1.42	0.08	0.65	1.04	51.00
$\sigma^{(1)}_{xx,avg}$=-2038.78	CFCF	0.85	0.91	1.34	1.02	1.18	1.17	02.00
$\sigma^{(1)}_{xx,avg}$=-1930.34	SSSS	0.16	1.07	1.75	1.57	1.38	1.39	21.00
$\sigma^{(1)}_{yy,avg}$=230.97	CCCC	1.55	0.82	1.10	1.78	1.66	1.33	16.00
$\sigma^{(1)}_{yy,avg}$=-63.71	CFCF	1.83	1.35	1.31	1.48	1.39	1.33	10.00
$\sigma^{(1)}_{yy,avg}$=-304.66	SSSS	0.47	0.83	1.39	5.22	1.26	1.41	09.00
$\sigma^{(1)}_{xy,avg}$=113.17	CCCC	1.43	0.80	1.11	1.61	1.47	1.35	17.00
$\sigma^{(1)}_{xy,avg}$=-73.46	CFCF	2.17	1.22	1.31	1.58	1.39	1.34	0.003
$\sigma^{(1)}_{xy,avg}$=-191.74	SSSS	0.35	0.84	1.33	8.09	1.20	1.43	11.00

Table 6: Quality of Estimator for $[-45/45/45/-45]$; plate dimension: $10 \times 10 \times 0.1$

Quantity	B. C.	$\kappa_{\mathcal{F}}$			% error
		E_1	E_2	E_3	
$\sigma^{(1)}_{xx,avg}$=-1880.40	SSSS	1.52	0.93	1.37	01.500
$\sigma^{(1)}_{yy,avg}$=-119.18	SSSS	0.06	0.69	1.17	79.400
$\sigma^{(1)}_{xy,avg}$=-97.99	SSSS	0.08	0.73	1.19	47.700
$\sigma^{(1)}_{xx,avg}$=1020.91	CCCC	0.71	0.68	1.18	25.800
$\sigma^{(1)}_{yy,avg}$=189.55	CCCC	45.43	0.87	1.04	05.000
$\sigma^{(1)}_{xy,avg}$=115.04	CCCC	5.24	0.85	1.08	04.200
$\sigma^{(1)}_{xx,avg}$=-994.24	CFCF	3.39	1.15	1.34	12.700
$\sigma^{(1)}_{yy,avg}$=-313.20	CFCF	0.28	0.55	1.09	32.900
$\sigma^{(1)}_{xy,avg}$=-176.08	CFCF	0.46	0.56	1.13	27.900

For the moderately thick plate (see table 7), we note that the error in the quantity of interest is small. Further, as observed above for the thin plate, estimator E_1 is unreliable while E_2 and E_3 are robust.

Remark: Estimator E_1 cannot be guaranteed to be reliable because $B(\mathbf{e}^*_{\mathbf{u}}, \mathbf{e}^*_{\mathbf{G}})$ need not be of the same sign as $B(\mathbf{e}_{\mathbf{u}}, \mathbf{e}_{\mathbf{G}})$ in each element of the current mesh. Thus, cancellation of error contributions from each element will not be properly accounted for by the

estimator. This can result in discrepancies in the estimated error. Estimator E_2 is more reliable because the sign of $B(\mathbf{e_u}, \mathbf{e_G})$ is not important in its definition.

Remark: Estimators E_2 and E_3 do a reasonable job of predicting the pollution error. Even though $\mathbf{e}^*_{\mathbf{G}}$ will not be reliable in region P, we find that the estimate (i.e. using $\mathcal{F}(\mathbf{e})$) is reasonably robust.

Since $\mid \mathcal{F}(\mathbf{e}) \mid_{E_1} \leq \mid \mathcal{F}(\mathbf{e}) \mid_{E_2} \leq \mid \mathcal{F}(\mathbf{e}) \mid_{E_3}$, it is important to find out how severe the over-estimation of the error can be when definition E_2 and E_3 are employed. In tables 8 and 9 we report the ratios $\mathcal{R}_1 = \mid \mathcal{F}(\mathbf{e}) \mid_{E_2} / \mid \mathcal{F}(\mathbf{e}) \mid_{E_1}$ and $\mathcal{R}_2 = \mid \mathcal{F}_2(\mathbf{e}) \mid_{E_2} / \mid \mathcal{F}_2(\mathbf{e}) \mid_{E_1}$, for the thin and thick plate with [0/90/90/0] stacking sequence. From tables 8 and 9 we observe that:

1 For the thin plate, where the error is significant, over-estimation due to definition E_2 of the error, is moderate with $\mathcal{R}_1 \leq 6$.

2 For the thick plate also, in general, over-estimation is moderate. For the case when $\mathcal{R}_1 \approx 150$, the actual error is very small (less than 0.003%). Thus, the over-estimated error also turns out to be very small.

3 The over-estimation depends on the plate thickness and boundary condition type.

4 In region P', the overestimation can be severe ($\mathcal{R}_2 > 15$ can be observed).

Table 7: Quality of Estimator for [0/90/90/0]; plate dimension: $10 \times 10 \times 1$

Quantity	B. C.	$\kappa_{\mathcal{F}}$			$\kappa_{\mathcal{F}_2}$			% error
		E_1	E_2	E_3	E_1	E_2	E_3	
$\sigma^{(1)}_{xx,avg}$=-2.26	CCCC	3.52	1.47	2.04	0.04	0.72	1.17	1.000
$\sigma^{(1)}_{xx,avg}$=-20.71	CFCF	30.69	1.07	1.75	0.59	0.74	1.18	0.003
$\sigma^{(1)}_{xx,avg}$=-14.87	SSSS	1.04	1.25	2.07	13.85	1.14	1.33	0.300
$\sigma^{(1)}_{yy,avg}$=2.76	CCCC	1.02	1.22	1.99	0.98	1.05	1.72	2.000
$\sigma^{(1)}_{yy,avg}$=-0.71	CFCF	0.04	1.28	2.01	0.61	1.54	1.95	0.800
$\sigma^{(1)}_{yy,avg}$=-3.34	SSSS	0.26	1.17	2.05	6.09	1.05	2.06	0.800
$\sigma^{(1)}_{xy,avg}$=0.97	CCCC	1.08	1.46	1.36	0.72	0.89	1.90	2.000
$\sigma^{(1)}_{xy,avg}$=-1.16	CFCF	0.13	1.41	1.59	0.51	1.36	1.85	0.300
$\sigma^{(1)}_{xy,avg}$=-2.34	SSSS	0.05	1.23	1.55	12.49	1.21	2.05	0.700

One-shot adaptivity for quantity of interest

In the previous section we presented the a-posteriori error estimators for the quantity of interest. Here, we will give an adaptive procedure by which the desired optimal mesh

Table 8: Over-estimation (definition E_2) for [0/90/90/0]; plate dimension: $10 \times 10 \times 0.1$

Quantity	B. C.	$\mathcal{R}_1$	$\mathcal{R}_2$
$\sigma^{(1)}_{xx,avg}$=-96.05	CCCC	5.85	1.42
$\sigma^{(1)}_{xx,avg}$=-2038.78	CFCF	1.82	3.07
$\sigma^{(1)}_{xx,avg}$=-1930.34	SSSS	1.65	8.66
$\sigma^{(1)}_{yy,avg}$=230.97	CCCC	1.92	1.95
$\sigma^{(1)}_{yy,avg}$=-63.71	CFCF	2.75	2.78
$\sigma^{(1)}_{yy,avg}$=-304.66	SSSS	3.23	17.28
$\sigma^{(1)}_{xy,avg}$=113.17	CCCC	1.88	1.75
$\sigma^{(1)}_{xy,avg}$=-73.46	CFCF	4.04	3.71
$\sigma^{(1)}_{xy,avg}$=-191.74	SSSS	2.34	32.02

Table 9: Over-estimation (definition E_2) for [0/90/90/0]; plate dimension: $10 \times 10 \times 1$

Quantity	B. C.	$\mathcal{R}_1$	$\mathcal{R}_2$
$\sigma^{(1)}_{xx,avg}$=-2.26	CCCC	9.49	1.24
$\sigma^{(1)}_{xx,avg}$=-20.71	CFCF	149.35	18.54
$\sigma^{(1)}_{xx,avg}$=-14.87	SSSS	6.27	207.46
$\sigma^{(1)}_{yy,avg}$=2.76	CCCC	1.72	1.81
$\sigma^{(1)}_{yy,avg}$=-0.71	CFCF	2.17	8.84
$\sigma^{(1)}_{yy,avg}$=-3.34	SSSS	2.44	14.19
$\sigma^{(1)}_{xy,avg}$=0.97	CCCC	2.23	1.28
$\sigma^{(1)}_{xy,avg}$=-1.16	CFCF	2.54	7.52
$\sigma^{(1)}_{xy,avg}$=-2.34	SSSS	2.47	31.97

can be obtained from an initial mesh computation directly. It will be shown in the subsequent section that the desired optimal mesh indeed leads to reduction of the error within specified tolerances.

Following [7], we can partition the contribution to the total error, $\mathcal{F}(\mathbf{e})$, into two parts $\mathcal{F}(\mathbf{e}) = \mathcal{F}_1(\mathbf{e}) + \mathcal{F}_2(\mathbf{e})$, as defined by (21). Following [6], we observe that the auxillary function $\mathbf{G}$ is unsmooth in P hence

$$|\mathcal{F}_1(\mathbf{e})| \leq \sum_{\tau \in P} ||\mathbf{e_u}||\,||\mathbf{e_G}|| \leq C\,h^p \tag{26}$$

where $||\mathbf{e_G}||$ does not converge at all (i.e. with a rate h^0). Beyond P, the auxillary function is well behaved and hence

$$|\mathcal{F}_2(\mathbf{e})| \leq \sum_{\tau \in P'} ||\mathbf{e_u}||\,||\mathbf{e_G}|| \leq Ch^{2p} \tag{27}$$

Thus, we have:

$$|\mathcal{F}(\mathbf{e})| \leq Ch^p \tag{28}$$

Remark: Using definition E_2 will ensure that the elements with higher intensity of contribution to total error are refined. This guarantees accuracy of pointwise quantities in a neighborhood of the region of interest. This is crucial in first-ply failure computation as location of the point also changes with the mesh, till convergence is achieved.

Remark: When reentrant corners are present in the domain, or when the plate model locks, the global part of the error, $\mathcal{F}_2(\mathbf{e})$, may be dominant and the rate of convergence can be much lower. However, for the adaptive strategy we will adopt the ideal a-priori estimates.

The goal of the adaptive process is to refine the given mesh selectively such that the total error is below the specified tolerance, i.e.

$$|\mathcal{F}(\mathbf{e})| \leq \eta\,|\mathcal{F}(\mathbf{u}_h)| \tag{29}$$

where $\mathcal{F}(\mathbf{u}_h)$ is the computed value of the desired quantity of interest; $|\mathcal{F}(\mathbf{e})| = |\mathcal{F}(\mathbf{e})|_{E_2}$ is obtained using definition E_2 for the error. Following [3], we will define $r_\tau = \frac{h_d}{h}$ as the ratio of the desired (h_d) to the actual mesh size (h) of the element τ. The desired mesh should have the least number of elements, of all possible meshes. Hence, following [3], we minimize

$$\sum_\tau \frac{1}{r_\tau^2}$$

subject to constraints (26) and (27). Thus, we define the new objective function (to be minimized) as,

$$J = \sum_{\tau} \frac{1}{r_\tau^2} + \lambda_1 (\sum_{\tau \in P} \chi_{d,\tau}^2 - \mathcal{F}_{d,1}) + \lambda_2 (\sum_{\tau \in P'} \chi_{d,\tau}^2 - \mathcal{F}_{d,2}) \tag{30}$$

where $\chi_{d,\tau} = |B(\hat{\mathbf{e}}_\mathbf{u}, \hat{\mathbf{e}}_\mathbf{G})|$ is the desired contribution to the total error from element τ; $\hat{\mathbf{e}}_\mathbf{u}, \hat{\mathbf{e}}_\mathbf{G}$ are the desired errors in the element τ; λ_1 and λ_2 are Lagrange multipliers; $\mathcal{F}_{d,1} = \eta_1 |\mathcal{F}(\mathbf{u}_h)|$ and $\mathcal{F}_{d,2} = \eta_2 |\mathcal{F}(\mathbf{u}_h)|$ are the desired errors in the region P and P', respectively (here $\eta = \eta_1 + \eta_2$). Using (26) and(27) $\chi_{d,\tau}^2$ can be given in terms of the actual error $\chi_{a,\tau}^2$ (where $\chi_{a,\tau}^2 = |B(\mathbf{e}_\mathbf{u}, \mathbf{e}_\mathbf{G})|$ in the element τ), as

$$\begin{aligned} &\text{For} \quad \tau \in P \quad \chi_{d,\tau}^2 = r_\tau^p \chi_{a,\tau}^2 \\ &\text{For} \quad \tau \in P', \quad \chi_{d,\tau}^2 = r_\tau^{2p} \chi_{a,\tau}^2 \end{aligned}$$

Thus, (30) becomes

$$J = \sum_{\tau} \frac{1}{r_\tau^2} + \lambda_1 (\sum_{\tau \in P} r_\tau^p \chi_{a,\tau}^2 - \mathcal{F}_{d,1}) + \lambda_2 (\sum_{\tau \in P'} r_\tau^{2p} \chi_{a,\tau}^2 - \mathcal{F}_{d,2}) \tag{31}$$

Minimizing J with respect to r_τ, λ_1 and λ_2 we get:
For $\tau \in P$,

$$r_\tau = \frac{\mathcal{F}_{d,1}^{1/p}}{(\sum_{\tau \in P} \chi_{a,\tau}^{4/(p+2)})^{1/p} \cdot \chi_{a,\tau}^{2/(p+2)}} \tag{32}$$

For $\tau \in P'$,

$$r_\tau = \frac{\mathcal{F}_{d,2}^{1/2p}}{(\sum_{\tau \in P'} \chi_{a,\tau}^{2/(p+1)})^{1/2p} \cdot \chi_{a,\tau}^{1/(p+1)}} \tag{33}$$

Using the computed values of r_τ, the desired mesh sizes can be computed. The mesh can be locally refined several times based on the desired mesh size. This leads to a final adaptively refined mesh.

Remark: The partition of the contribution to the error from P and P' is based on the user. The final mesh depends on the choice of η_1 and η_2. In order to keep both contributions of the same order, we choose $\eta_1 = \eta_2 = \eta/2$.

Numerical Examples using one-shot focussed adaptivity

The adaptive procedure given above can be employed to selectively refine the initial mesh, in order to get the desired mesh (with error in the quantity of interest within the

specified tolerance) in one shot. The computation has to be redone on the final mesh in order to obtain the quantity of interest. Below, we will demonstrate through numerical examples, for the thin plate, the effectiveness of this two-mesh solution process.

Let us consider the laminate configuration (thin plate) given previously. For this laminate, the [0/90/90/0] and [-45/45/45/-45] stacking sequences are taken. For the adaptive procedure we let the specified tolerance for the error in the quantity of interest be $\eta = 3\%$ error. For the initial mesh shown in figure 6, we let $\sigma^{(1)}_{xx,avg}$ and $\sigma^{(1)}_{yy,avg}$ (i.e. average stress components in the topmost layer) be the quantity of interest, for the element τ shaded gray. In figure 7 we show the final meshes obtained by the adaptive process, using definition E_2 of the pointwise error estimator. In table 10 the details of the material, quantity of interest, errors in the initial mesh ($\|\mathcal{F}(\mathbf{e})\|_{in}$) and the final mesh ($\|\mathcal{F}(\mathbf{e})\|_{fin}$), and the tolerance achieved ($\eta_{achieved}$) are reported for the meshes shown in figure 7. From the results we note that:

(1) The final meshes in all the cases correspond to an error within the specified tolerance ($0.013 \leq \eta_{achieved} \leq 0.037$).

(2) The final mesh depends strongly on the quantity of interest, ply orientations and the boundary-conditions.

(3) The region of strong refinements is not restricted to the local region of interest only. It can spread to a larger part of the initial mesh, depending on the quantity of interest, boundary-conditions and material orientation.

(4) Almost the full mesh requires further refinements.

As a check, the quality of the error estimator (using definition E_2) for the final mesh 6, was obtained. The effectivity index was found to be $\kappa_{\mathcal{F}} = 0.70$. The true error in the quantity was $1.368\,KPa$, i.e. an error of less than 0.1%.

Adaptivity for a domain with a cut-out

Generally composite panels, employed in practical applications, have cut-outs (for window openings, inspection bays, or for weight saving). In order to study the effect of cut-outs on the adaptive process, we consider the domain of figure 8, with a triangular cut-out. For this domain, the initial mesh is as shown in figure 8. As detailed in table 12, the final meshes were obtained for various combinations of quantities, boundary conditions and ply-orientations. Results for both $p = 2$ and $p = 3$ have been reported,

Table 10: One-shot adaptivity for control of error in quantity of interest: Definition E_2 for the error in quantity; average stress in the topmost layer, in the element τ (shown shaded gray in figure 6); Errors in the initial and final (adaptively refined) meshes.

Mesh	Laminate	Quantity	$\lvert\mathcal{F}(\mathbf{e})\rvert_{init}$	$\lvert\mathcal{F}(\mathbf{e})\rvert_{fin}$	$\lvert\mathcal{F}(\mathbf{u}_h)\rvert$	$\eta_{achieved}$
1	[0/90/90/0] (SSSS)	$\sigma^{(1)}_{xx,avg}$	649.56	39.32	1558.36	0.025
2	[0/90/90/0] (SSSS)	$\sigma^{(1)}_{yy,avg}$	86.77	9.67	283.01	0.034
3	[0/90/90/0] (CFCF)	$\sigma^{(1)}_{yy,avg}$	18.03	0.75	57.66	0.013
4	[-45/45/45/-45] (SSSS)	$\sigma^{(1)}_{xx,avg}$	331.83	44.69	1933.11	0.023
5	[-45/45/45/-45] (CFCF)	$\sigma^{(1)}_{yy,avg}$	97.61	9.43	421.05	0.022
6	[-45/45/45/-45] (CFCF)	$\sigma^{(1)}_{xx,avg}$	613.09	31.31	834.63	0.037

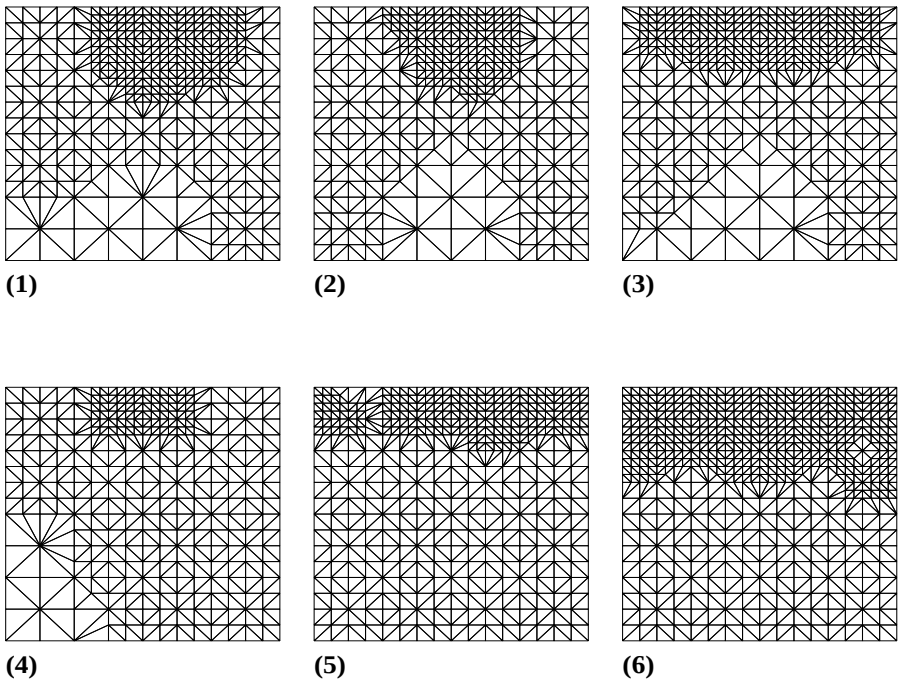

Figure 7: One-shot adaptivity: Definition E_2 for the error; the final meshes obtained for various choices of quantities of interest, boundary-conditions and material orientations in each lamina

for the element τ shown shaded gray in figure 8 for the topmost layer (i.e. $l = 1$). From Table 12 we note that:

(1) For $p = 2$ the desired tolerance is achieved with significantly higher number of degrees of freedom, as compared to $p = 3$.

(2) Even for $p = 3$, the given initial mesh was not sufficient, leading to a significantly refined final mesh.

(3) The final meshes are very sensitive to the quantity of interest, ply-orientations, and boundary conditions.

(4) Refinement near the corners of the cut-out depends on the quantity of interest, boundary-condition and the ply-orientations. Refinements near the cut-out can be significant even for $p = 3$. This is because of stress concentrations arising at the corners of the cut-outs.

(5) The desired levels of refinement is not the same at each of the corners of the cut-out. The desired level depends on the quantity, material orientation and boundary conditions.

(6) The value of $\eta_{achieved}$ is generally higher than 0.03.

The higher final tolerance is due to the fact that the corners in the cut-out cause a suboptimal rate of convergence of the finite element solution. Thus, the desired mesh sizes, obtained using the optimal rate of convergence, are higher than the true one. However, a further iteration of the refinement process will lead to the desired mesh. Note that, inspite of the restrictive assumption on the rate of convergence, the mesh obtained is always close to the desired one. Hence, the one-shot adaptive refinement procedure is very effective.

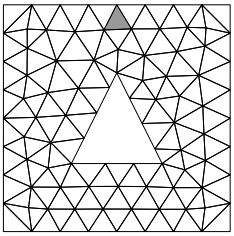

Figure 8: One-shot adaptivity: The initial mesh for domain with cut-out; element of interest τ shown shaded gray.

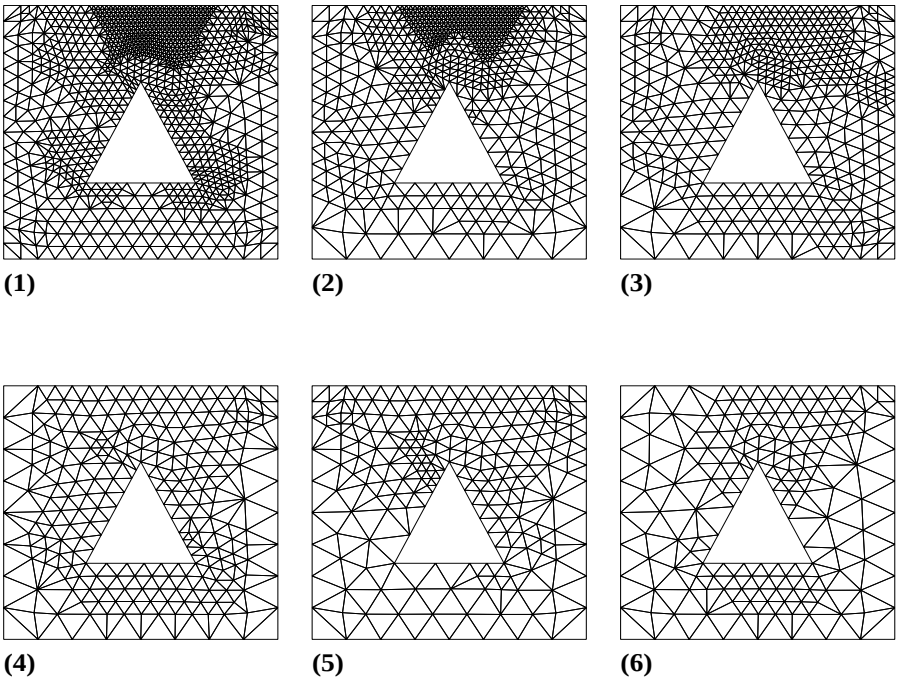

Figure 9: One-shot adaptivity: Definition E_2 for error in quantity; average stress in topmost layer for element shown shaded gray in figure 5; the final meshes obtained for various choices of quantities of interest, boundary-conditions and material orientations in each lamina (see table 10 for the details). Meshes 1,2 and 3 correspond to $p = 2$; the corresponding final meshes for $p = 3$ are given by meshes 4, 5 and 6 respectively.

Table 11: Effect of order of approximation: Definition E_2 for error in quantity; average stress in the topmost layer, in the element τ (shown shaded gray in figure 3); errors in the initial and final (adaptively refined) meshes for $p = 3$. The quantities in parentheses in the last column correspond to the final mesh for $p = 2$.

Mesh	Laminate	Quantity	$\lvert\mathcal{F}(\mathbf{e})\rvert_{in}$	$\lvert\mathcal{F}(\mathbf{e})\rvert_{fin}$	$\eta_{achieved}$	No. of DOFs
1	[0/90/90/0] (SSSS)	$\sigma^{(1)}_{xx,avg}$	24.4	24.4	0.016	625×8 (1520×8)
2	[0/90/90/0] (SSSS)	$\sigma^{(1)}_{yy,avg}$	10.2	0.8	0.003	967×8 (1429×8)
3	[-45/45/45/-45] (CFCF)	$\sigma^{(1)}_{xx,avg}$	70.9	20.0	0.024	1330×8 (2264×8)

Table 12: One-shot adaptivity for a domain with a cut-out: Effect of order of approximation; definition E_2 for error in quantity; average stress in the topmost layer, in the element τ (shown shaded gray in figure 5); errors in the initial and final (adaptively refined) meshes for $p = 2, 3$.

Mesh	p	Laminate	Quantity	$\lvert\mathcal{F}(\mathbf{e})\rvert_{in}$	$\lvert\mathcal{F}(\mathbf{e})\rvert_{fin}$	$\eta_{achieved}$	No. of DOFs
1	2	[0/90/90/0] (SSSS)	$\sigma^{(1)}_{yy,avg}$	85.4	2.46	0.021	4096×8
2	2	[0/90/90/0] (CCCC)	$\sigma^{(1)}_{xx,avg}$	94.0	5.7	0.041	2673×8
3	2	[-45/45/45/-45] (CFCF)	$\sigma^{(1)}_{yy,avg}$	126.1	15.9	0.031	1777×8
4	3	[0/90/90/0] (SSSS)	$\sigma^{(1)}_{yy,avg}$	31.7	4.7	0.041	2088×8
5	3	[0/90/90/0] (CCCC)	$\sigma^{(1)}_{xx,avg}$	29.0	6.1	0.045	1821×8
6	3	[-45/45/45/-45] (CFCF)	$\sigma^{(1)}_{yy,avg}$	18.3	7.6	0.015	1422×8

Conclusion

(1) Estimators EST1, EST3 and EST4B are very reliable for interior patches

(2) Explicit imposition of the applied Dirichlet boundary conditions, inthe recovered displacement field, improves the quality of the estimator EST3

(3) Explicit imposition of the applied Dirichlet boundary conditions, inthe recovered displacement field, improves the quality of the estimator EST3

(4) The behavior of the estimators is relatively insensitive to the higher order plate model used.

(5) For the displacement-based recovery procedure, $p + 2$ order recovery is preferable, as compared to $p + 1$ order recovery.

(6) The estimation of the error in the local quantity of interest requires computation of the solution corresponding to an auxillary problem. This leads to an additional load-vector for the standard finite element computations.

(7) Employing a L_2-recovery based error estimator, quick and reliable estimates of the error in the quantity of interest can be obtained

(8) The adaptive algorithm employs the partitioning of the contribution to the total error, in the quantity of interest, into local and far-field components.

(9) The meshes obtained depend strongly on the boundary-conditions, material orientation and the quantity of interest.

References

[1] Abrate S. Optimal design of laminated plates and shells. Composite Struct. 1994;29:269-286.

[2] Babuska I, Strouboulis T, Upadhyay CS, Gangaraj SK. A posteriori estimation and adaptive control of the pollution error in the h-version of the finite elementmethod. Int. J. Numer. Methods Eng. 1995; 38:4207-4235.

[3] Ladeveze P, Pelle JP, Rougeot PH. Error estimation and mesh optimization for classical finite elements. Engg. Computations 1991; 8:69-80.

[4] Verfurth R. A review of a-posteriori error estimation and adaptive mesh-refinement. Wiley Tuebner, New York 1996.

[5] Babuska I, Strouboulis T, Upadhyay CS, Gangaraj SK. A Posteriori estimation and adaptive control of the pollution error in the h version of the finite element method. Int. J. Numer. Methods Engg. 1995; 38:4207-4235.

[6] Wahlbin LB. Local behavior in finite element methods, in Handbook of Numerical Analysis, (Vol. II) Ciarlet PG, Lions JL, eds. North Holland 1991; 357-521.

[7] Babuska I, Strouboulis T, Mathur A, Upadhyay CS. Pollution error in the h version of the finite element method and the local quality of a-posteriori error estimators. Finite Elements in Analysis and Design 1994; 17:273-321.

[8] Actis RL, Szabo BA, Schwab C. Hierarchic models for laminated plates and shells. Comput. Methods Appl. Mech. Engg. 1999; 172:79-107.

[9] Kapania RK, Raciti S. Recent advances in analysis of laminated beams and plates, Part I: shear effects and buckling. AIAA Journal 1989; 27(7):923-934.

[10] Zhu JZ, Zienkiewicz OC. Superconvergence recovery technique and a posteriori error estimators. Int. J. Numer. Methods Eng. 1990; 30:1321-1339.

[11] Babuska I, Strouboulis T, Gangaraj SK, Upadhyay CS. Validation of recipes for the recovery of stresses and derivatives by a computer-based approach. Mathl. Comput. Modelling 1994; 20:45-89.

[12] Babuska I, Strouboulis T, Upadhyay CS. A model study of the quality of a posteriori error estimators for linear elliptic problems. Error estimation in the interior of patchwise uniform grids of triangles. Comput. Methods Appl. Mech. Engg. 1994; 114:307-378.

[13] Zienkiewicz OC, Zhu JZ. Error estimates and adaptive refinement for plate bending problems. Int. J. Numer. Methods Eng. 1989; 28:2839-2853.

[14] Reddy YSN, Reddy JN. Linear and non-linear failure analysis of composite laminates with transverse shear. Composites Science and Technology 1992; 44:227-255.